Analysis of mutations in EF-G that confer resistance to aminoglycosides.

THESIS

Presented in Partial Fulfillment of the Requirements for the Degree Master of Science in the Graduate School of The Ohio State University

By

Stephen McGarry

Graduate Program of Biochemistry

The Ohio State University

2022

Master's Examination Committee:

Professor Jane Jackman, Advisor

Professor Kurt Fredrick

Abstract

The ribosome is a universally conserved RNA-based machine that uses mRNA as a template to make proteins, in a process known as translation. Translation occurs in 4 steps: initiation, elongation, termination, and ribosome recycling. The elongation phase of translation entails a cycle of three main events for each amino acid incorporated into the nascent chain: decoding, peptidyl transfer, and translocation. During translocation, elongation factor G (EF-G) binds the 70S ribosome, hydrolyzes GTP, and disrupts interactions between the codon-anticodon helix and the 30S A site. This in turn promotes movement of the tRNAs from the A/P and P/E sites into the chimeric ap/P and pe/E sies while preventing backwards movement of the tRNAs. As translocation completes, the A-site tRNA is moved fully into the P site, the P-site tRNA is moved fully into the E site, and the mRNA has shifted by 3 base pairs. Elongation is a prime target for antibiotic-based therapies, as disrupting elongation has the effect of preventing protein synthesis and generating miscoded or prematurely terminated proteins. Aminoglycosides (AGs) represent one class of antibiotics capable of these interactions. AGs function by binding h44, occluding residues A1492 and A1493, and stabilizing tRNA in the A site. Recently, researchers have found that mutations in domain 4 of EF-G appear to confer low levels of resistance to AGs *in vivo.*

In the present study, I investigate the basis of this effect with *in vitro* protein synthesis assays. I purified each mutant EF-G identified and tested them in an *in vitro* protein expression system. Using ^{35}S for imaging, and a variety of AG concentrations, I was able to calculate the IC_{50} for each mutant EF-G. Ultimately, I did not find a significant difference in IC_{50} between the WT and any of the mutants. The simplest interpretation of these results is that the mutations act indirectly to confer AG resistance *in vivo*.

Acknowledgements

I would like to thank Dr. Kurt Fredrick for accepting me into his lab and advising me throughout my time at OSU. I would also like to thank Dr. Jane Jackman for agreeing to be my advisor on short notice. To my family and to my lab mates, thank you for helping and encouraging me.

Vita

Born……March 3rd, 1998

2016……International School of Beaverton

2020…….. B.A. Biochemistry, College of Wooster

2020 to present…….....Graduate Research Associate, Department of Chemistry and Biochemistry, The Ohio State University

Publications

Vicker, S. L.; Maina, E. N.; Showalter, A. K.; Tran, N.; Davidson, E. E.; Bailey, M. R.; McGarry, S. W.; Freije, W. M.; West, J. D. Broader than Expected Tolerance for Substitutions in the WCGPCK Catalytic Motif of Yeast Thioredoxin 2. *Free Radic. Biol. Med.* **2022**, *178*, 308–313. https://doi.org/10.1016/j.freeradbiomed.2021.09.009.

Major Field: Biochemistry

Table of Contents

List of tables

List of figures

Chapter 1: Introduction

1.1 The Ribosome

The ribosome is an RNA-based machine responsible for protein synthesis in every living cell. In bacteria, the fully assembled ribosome (70S) consists of two subunits: the large 50S subunit and the small 30S subunit. The 50S subunit functions to catalyze peptide bond formation and is composed of the 5S ribosomal RNA (rRNA), the 23S rRNA, and about 30 proteins[1]. The 30S subunit serves to bind and position messenger RNA (mRNA) and consists of the 16S rRNA and about 20 proteins[1]. When the two subunits come together to make the 70S ribosome, three transfer RNA (tRNA) binding sites are formed: the aminoacyl or A site, the peptidyl or P site, and the exit or E site (figure 1.1).

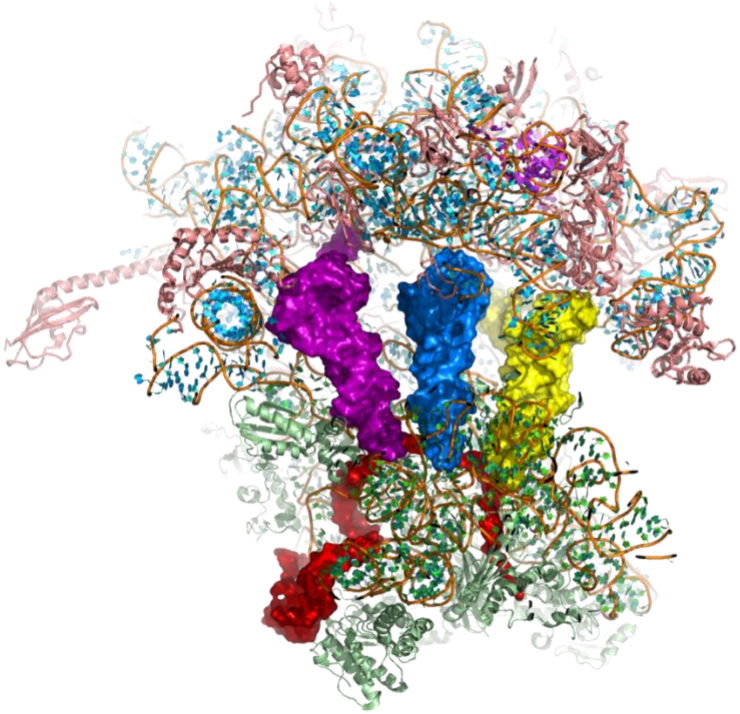

Figure 1.1: Structure of the 70S ribosome with tRNA. The color identification for the different molecular components are: 16S rRNA, green; 23S rRNA, cyan; 5S rRNA, magenta; 30S proteins, light green; 50S proteins, light pink; mRNA, red; A site Phe-tRNA, yellow; P site fMet-tRNA, dark blue; E site tRNA, dark purple. (Adapted from Yusupova et. al 2015[2]).

The 70S ribosome functions as an enzyme and catalyzes translation, a process in which proteins are built according to an mRNA template. Translation occurs in four main stages: initiation, elongation, termination, and ribosomal recycling. Initiation involves the assembly of a ribosome complex at the start codon (AUG, UUG, or GUG) of mRNA and begins with the binding of initiation factor 3 (IF3) to the 30S subunit. IF3 serves to block the 50S from forming a complex with the 30S until the mRNA, tRNA, and other factors have bound[3]. The 30S-IF3 forms a complex with IF1 and IF2 before binding mRNA and formyl methionyl initiator tRNA (fMet-tRNA^{fMet}). In most bacteria, in order to position mRNA correctly, the 30S subunit engages the Shine-Dalgarno (SD) sequence. The SD sequence is a region of mRNA with the consensus sequence 5'AGGAGG-3'[4]. The 3' end of 16S rRNA contains the anti-Shine-Dalgarno (aSD) sequence which base pairs with the SD[4,5]. The pairing of aSD and SD positions the start codon in the 30S P site where fMet-tRNA^{fMet} binds[4]. This mechanism also prevents internal methionine codons from being recognized as start codons. IF2 is a GTPase that functions to recruit the fMet-tRNA^{fMet} to the P site while discriminating against elongator tRNAs[6]. IF1 binds to the A site where it prevents aminoacyl tRNAs from binding and stabilizes the other initiation factors[7]. This complex, known as the 30S initiation complex (30SIC), docks with the 50S and sheds IF3, triggering IF2 to hydrolyze GTP. IF1 and IF2 also dissociate, creating the 70SIC and completing initiation[8,9].

The elongation phase of translation entails a cycle of three main events for each amino acid incorporated into the nascent chain: (1) decoding, (2) peptidyl transfer, and (3) translocation. The first event of elongation is decoding, also termed aminoacyl-tRNA (aa-tRNA) selection. This step begins with the formation of the ternary complex: elongation factor thermo unstable (EF-Tu), an aa-tRNA, and GTP. Once this complex forms it binds to the ribosome near the A site[10]. If codon-anticodon base pairing occurs, EF-Tu hydrolyzes GTP, the acceptor end of the aa-tRNA moves

into the 50S A site, and EF-Tu dissociates[11]. Once aa-tRNA moves into the 50S A site, peptidyl transfer occurs. In this step, the P and A loops of the 50S subunit position the two tRNAs so that the amino group of the A site tRNA can attack the peptide chain, transferring the peptide to the A-site tRNA[12]. In the final step of elongation, known as translocation, the tRNAs move to their adjacent sites along with paired mRNA. The tRNAs move in a stepwise manner, with the acceptor arms of the tRNA moving first with respect to the 50S, reaching the A/P and P/E hybrid sites[13]. This movement can occur spontaneously but often is facilitated by the binding of elongation factor G (EF-G) and GTP to the ribosome. EF-G is an essential prokaryotic translation factor with a mass of 76.4 kilodaltons, contains GTPase activity, and is responsible for catalyzing the movement of mRNA and tRNA from the A site to the P site[14]. EF-G consists of 5 domains which can be categorized into two super domains: the fixed domain (I-II), and the mobile domain (III, IV, V) (figure 1.2)[15].

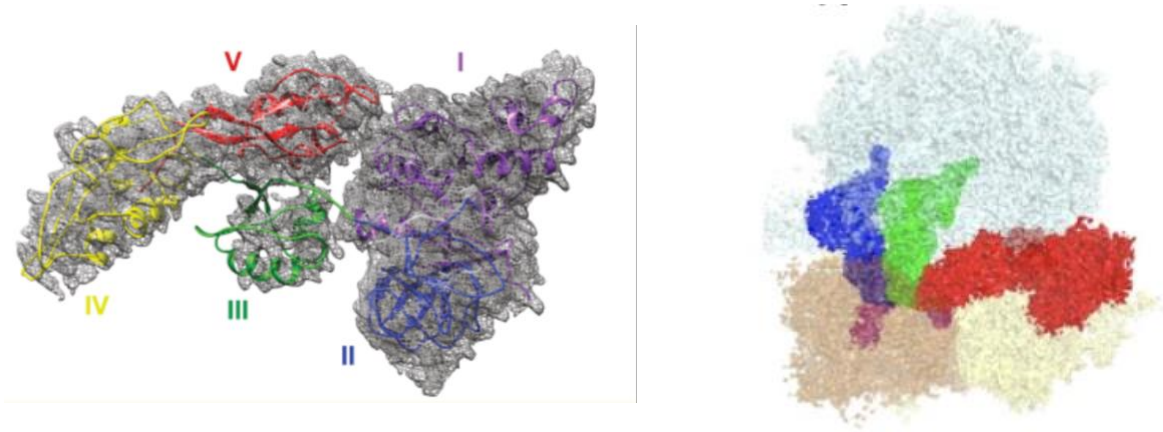

Figure 1.2: Overview of EF-G. The left figure displays EF-G in the POST state. Domains are labeled and color coded 1-5[16]. Domain 1 is responsible for GTPase activity. The right figure displays a cryo-EM density map of the POST state of EF-G (in red) bound to a 70S ribosome[17]. In blue and green are the tRNAs in the E and P site respectively. (Adapted from Macé, K et. al 2018[16] and Carbone et. al 2021[17])

Upon binding, EF-G hydrolyses GTP and experiences a conformational change disrupting the interactions between the codon-anticodon helices of the 30S subunit, enabling rapid movement of the mRNA by three base pairs, the translocation of the A/P tRNA to the P site, and the P/E tRNA to the E site[18]. EF-G then dissociates, and the elongation cycle repeats until the ribosome reaches a stop codon.

Termination of protein synthesis occurs when a stop codon (UAG, UAA, or UGA) enters the A site of a translating ribosome. When a stop codon enters the A site, one of two release factors recognize the codon and bind in between the 50S and 30S in the A site, releasing the nascent peptide via a GlyGlyGln motif that promotes hydrolysis of the ester bond of the P-site peptidyl-tRNA[19]. UAG and UAA codons are recognized by release factor 1 (RF1) via a conserved ProGluThr motif, while RF2 recognizes the UGA and UAA codons via a conserved SerProPhe motif[20]. After peptidyl-tRNA hydrolysis, RF1 and RF2 dissociate from the ribosome, a process that is dependent on RF3[21]. RF3-GTP binds to a region known as the interphase cavity where it undergoes a conformational change that promotes dissociation of RF1/2[22]. RF3 hydrolyses GTP in the process, and then dissociates.

Ribosome recycling is the process of dissociating the mRNA and P-site tRNA from the 70S and splitting the 70S into subunits. The mechanism of ribosome recycling is not well understood; however, it is known that EF-G and ribosome recycling factor (RRF) are necessary[23,24]. As these two proteins bind, the ribosome rotates, disrupting bridges B2a and B3[25]. The exact order can vary, but generally the destabilization of these bridges lowers the energy barrier for dissociation, allowing the mRNA, then the P-site tRNA to dissociate[26,27]. Finally, the 30S and 50S subunits dissociate in an EF-G and RRF-independent reaction. The 30S subunit binds

IF3, and the mRNA, tRNA and ribosomal subunits are recycled for use in another round of translation[26].

1.2 An overview of EFG and translocation

After peptidyl transfer, the 70S ribosome contains a peptidyl-tRNA in the A site and a deacyl tRNA in the P site. This is known as the classical state with tRNAs in the P/P and A/A sites. However, the classical state is not inherently stable and will spontaneously convert to the hybrid state. The 30S subunit rotates 10.7°, shifting the acceptor arm of the deacyl tRNA into the 50S E site while the anticodon stem-loop remains in the 30S P site[13], hence occupying the P/E site. The peptidyl-tRNA shifts its acceptor arm into the 50S P site while its anticodon arm remains in the 30S A site, occupying the A/P site (figure 1.3)[28,13]. Movement of the tRNAs into hybrid sites is accompanied by intersubunit rotation and 30S head swiveling.

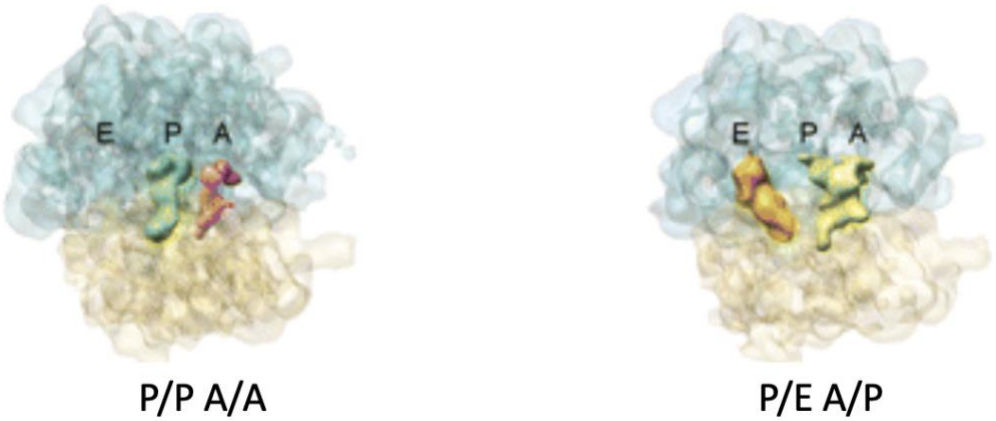

Figure 1.3: Hybrid state model of translocation. 3D density maps prepared via cryo-EM analysis of pre-translocation 70S ribosomes. On the left is a ribosome in the classical state with $tRNA^{fMet}$ bound to the A/A and $tRNA^{Leu}$ bound to the P/P site. On the right is a ribosome in a hybrid state with $tRNA^{fMet}$ in the P/E and $tRNA^{Leu}$ in the A/P sites. Hybrid state ribosomes shift acceptor arms of the tRNA into the adjacent 50S site while the anticodon arm remains in the 30S[28]. (Adapted from Julián et. al 2008[28]).

Once the ribosome adopts the hybrid state it becomes an ideal substrate for EF-G. As EF-G fully engages the complex, several processes occur. Firstly, EF-G experiences a conformational change, extending to a length of about 100 Å[17]. Secondly, the different domains of EF-G bind to different parts of the ribosome. The GTPase domain (domain 1) binds to the sarcin-ricin loop (SRL) and becomes clamped in place by the 30S and 50S[16]. Domain 5 binds to the L11 stalk of the 50S while domains 2 and 3 bind near the 30S shoulder and 30S head. As domain 1 binds to the SRL, switch loops (SW) stabilize the GTP binding pocket[17]. SW-1 accomplishes this by docking His44 to G2655 of the SRL, while the catalytic His92 of SW-2 docks with a its side chain orientated towards the gamma phosphate of GTP[17,29]. During binding, GTP is hydrolyzed, and the Pi is retained. The stabilization provided by the switch loops, the 30S rotation, and magnesium ions prevents PI release and EF-G dissociation. Domain 4 is inserted between the peptidyl tRNA, the 30s head, and the 30S shoulder. The tip of domain 4, known as loop 1, becomes wedged near the 16S nucleotide G530 which is universally conserved and essential for mRNA decoding and tRNA stabilization in the A site[30]. This has the effect of positioning domain 4 to separate the codon-anticodon helix from the A site decoding center[17].

Next, the 30S body reverses its rotation by about 5 degrees while the 30S head rotates about 17 degrees[31]. This has the effect of partially separating domain 1 from the SRL and allowing Pi to be released. Furthermore, EF-G prevents reverse movement of the peptidyl tRNA to the A/A state during the reverse rotation. While domains 1 and 2 loosen their grip on the ribosome, EF-G remains bound by domains 4 and 5. This rotation causes domains 2, 3, and 4 to move along the 30S. Domain 4 slides 20 Å and becomes fully inserted into the A site[17]. Loop 1 is now in direct contact with the codon-anticodon nucleotides where is separates tRNA from the decoding center. This causes the deacyl tRNA, peptidyl tRNA, and the mRNA to translocate 18 Å into the ap/P and pe/E chimeric

hybrid states. In this state, U34 of the anticodon loop stacks with C1400 of the 16S P site[17,32]. Chimeric hybrid states indicate that the acceptor arm of the tRNA is interacting with sites from both the original site and the site it is translocating to. Despite this movement, the peptidyl tRNA and deacyl tRNA have not fully translocated as the 17-degree rotation of the 30S head increases the distance the tRNAs need to travel.

The next step of translocation involves the 30S body of the ribosome reversing its rotation by another 1.1 degrees while the head rotates a further 1.1 degrees[17,31]. This has the effect of shifting domain 4 of EF-G another 4Å along the mRNA. Both the peptidyl tRNA and the deacyl tRNA are deep in their respective 30S sites, however they have not translocated yet. At this point EF-G begins dissociating from the ribosome. Domain 3 remains loosely bound while Domain 1 fully releases the SRL and domain 2 exits the 30S subunit, preventing clash with protein S12[17,24]. The dissociation of EF-G is stepwise and similar to that of EF-Tu as the GTPase domain is released first. Upon binding, domain one had a surface area with the SRL equal to about 960 $Å^2$. During the 20 Å shift of domain 4 this area decreases to about 493 $Å^2$, before completely dissociating in this step[17]. In contrast, domain 5, which was bound to stalk L11, maintains a surface area of about 900 $Å^2$ throughout all steps while domain 4 experiences a rise in surface area as it shifts into the A site and down the ribosome. Upon binding domain 4 had a surface area of about 800 $Å^2$ however this rose to 1440 $Å^2$ by the time it fully occupied the A site[17]. Despite the increase in surface area of domain 4, with each step of translocation EF-G as a whole loses surface area, and by the end of this reaction it will dissociate fully.

Despite the fact that EF-G has dissociated, translocation is not complete. The deacyl tRNA and peptidyl tRNAs remain deep in the pe/E and ap/P transition states. In order to complete the reaction the 30S head has to swivel in reverse 20 degrees back to its unrotated state[31,17,33]. When

this occurs the peptidyl tRNA shifts with the mRNA fully into the P/P site, and the deacyl tRNA shifts into the E/E, site from which it can dissociate.

1.3 Aminoglycosides

Elongation involves a repeated cycle and is a prime target for antibiotic-based therapies. Halting or disrupting elongation has the effect of preventing protein synthesis and generating miscoded or prematurely terminated proteins. One class of antibiotics that inhibit elongation are aminoglycosides (AGs). AGs are composed of an aminocyclitol ring linked to various amino sugars by glycosidic bonds[34]. While they are broad spectrum antibiotics, AGs are more effective against gram negative bacteria. The primary binding site of AGs is helix 44 (h44) of the 16S rRNA, near the A site of the 30S subunit (figure 1.4)[35].

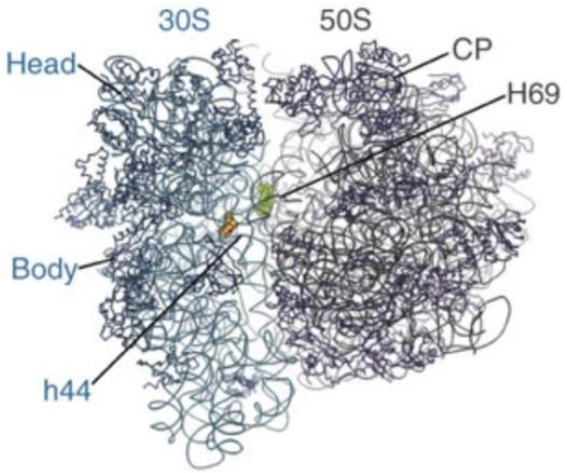

Figure 1.4: Binding sites of aminoglycosides. The AG Neomycin bound to h44 in the 30S A site and H69 of the 50S subunit. Binding of AGs to these sites inhibits translocation, promotes miscoding, and inhibits ribosome recycling[35]. (Adapted from Borovinskaya et. al 2007[35]).

When AGs bind to this site, ring 1 inserts itself into h44, stacking with G1491 and hydrogen bonding with A1408. This in turn occludes residues A1492 and A1493, "flipping" them out of

h44, a process that normally occurs upon codon-anticodon base pairing[34]. This stabilizes tRNA binding to the A site by reducing the energy barrier for flipping A1492 and A1493, which in turn promotes near cognate and cognate tRNA binding, causing miscoding errors and inhibiting translocation. Structural studies identified another AG binding site in helix H69 of the 50S subunit. H69 forms an inter-subunit bridge through contacts with nucleotides 1406-1409 and 1494-1495 of the 16S rRNA[34]. Some data suggests that AGs bound to H69 are able to stabilize the inter-subunit bridge and prevent separation of the two subunits by RRF and EF-G, further inhibiting translation, although the h44 site is of primary relevance *in vivo*[35].

Bacteria have evolved various mechanisms of resistance to AGs. When a cell evolves resistance to an antibiotic, it normally uses one or more of the following mechanisms: (1) efflux pumps, (2) chemical inactivation of the antibiotic, (3) chemical modification of the target or (4) protection of the drug target[36]. Efflux pumps such as the MexX-MexY channels in *Pseudomonas aeruginosa* use active transport to bind to and eject kanamycin. Specialized acetyltransferases modify AGs, inhibiting their ability to bind to the 30S subunit [37,38]. These forms of resistance are widespread in nature due to the fact they are transferrable. This means that the organism can transfer resistance in ways other than direct reproduction: most commonly through horizontal gene transfer. During horizontal gene transfer, DNA is moved from one microorganism to another via uptake of naked DNA (transformation), plasmid-mediated transfer (conjugation) or phage-mediated transfer (transduction)[39].

One type of transferrable resistance relevant to EF-G is ribosomal protection provided by tetracycline resistance protein O (Tet-O). Tet-O is an elongation factor like protein that provides cells with lasting protection against tetracycline. Due to its 50% sequence similarity with EF-G, the retained GTPase activity of domain 1, and similar structure to EF-G, it is believed that Tet-O

has evolved from a duplicate EF-G gene[40]. Tetracycline is a broad-spectrum antibiotic composed of a fused linear tetracycline core that binds to the 30S A site, where it prevents codon-anticodon base pairing and tRNA binding[41]. After tetracycline binds to the A site, Tet-O binds to the 70S ribosome much like EF-G, hydrolyzing GTP, and inducing a conformational change in helix 34 and nucleotides 1209 and 1054 of the 30S.[40] These reorganizations of the 30S disrupt the hydrogen bonds responsible for tetracycline binding, ejecting tetracycline from its site[40]. After Tet-O dissociation, EF-Tu dependent decoding can occur, and elongation can resume.

Recently, researchers have found that when different bacteria like P*seudomonas aeruginosa*, *Escherichia coli*, and *Acinetobacter baumannii* were grown in sublethal concentrations of aminoglycosides such as kanamycin, tobramycin, and gentamycin, they quickly evolved into fast-growing variants with point mutations in EF-G[42,43]. *In vivo*, these mutations appear to confer low levels of resistance, permitting bacteria to grow in concentration 2- to 4- fold higher than could otherwise be tolerated[44]. Five mutations were commonly identified in different species of bacteria with various aminoglycosides: F593L, F605I, F605L, A608E, and P610T [42,43,44]. These mutations are all located in domains three and four of EF-G, which are the domains that undergo the largest conformational change and physically contact the tRNAs.

I wondered if these mutations enable EF-G to act as ribosome protector by promoting dissociation of AGs, akin to the mechanism of Tet-O. If so, they could illuminate a potential path in the evolution of transferrable resistance factors like Tet-O. To investigate this, I tested whether the AG resistance seen *in vivo* could be replicated *in vitro*. Through inhibitory concentration assays, I found that the mutant EF-Gs do not significantly protect translation from aminoglycosides. This suggests that that these EF-G mutations are not directly responsible for the observed resistance *in vivo*, and they likely play an indirect role in providing resistance.

Chapter 2: Analysis of EF-G variants that confer AG resistance

2.1 Introduction

It has been shown that certain mutations in EF-G confer a small increase in AG resistance, however, the mechanism behind this resistance is unknown. One potential explanation is that the mutations in domain 4 of EF-G alter the conformational dynamics of EF-G, allowing it to expel the AG or disrupt the inhibitory interactions caused by the AG.

To investigate whether these mutations are directly responsible for the *in vivo* resistance, I calculated the half maximal inhibitory concentration (IC_{50}) of the mutant EF-Gs *in vitro*. I measured protein synthesis *in vitro* in the presence of increasing AGs concentrations, using the Protein synthesis Using Recombinant Elements (PURE) system (NEB), which contains all the necessary cellular machinery for transcription (T7 RNA polymerase, AMP, GMP, CMP, UMP), translation (70S ribosomes, IF1-3, EF-Tu, EF-T, EF-G, RF1-3, RRF), energy regeneration (ATP, GTP, UTP, CTP, creatine phosphate, creatine kinase, myokinase, nucleoside diphosphate kinase, pyrophosphatase), and aminoacylation (all 20 aminoacyl tRNA synthases). A custom kit lacking EF-G was ordered so our mutant varieties could be used.

2.2: Materials and methods

2.2.1: Mutagenesis and transformations

All five EF-G mutants were created via Phusion Site Directed Mutagenesis, a process which uses phosphorylated primers to create point mutations in a plasmid. The DNA template used was the protein expression vector pET24b containing the wild type *E.coli* EF-G gene. A 50 μL PCR reaction containing 1x Phusion buffer, 200 μM dNTPs, 0.5 μM forward and reverse primers, 0.02 U/μL Phusion polymerase, 100 ng/μL template DNA (pET24b-EFG-His6), and 3% DMSO generated linear copies of the plasmid which contained a given mutation. These products were ligated and then transformed into competent DH5α cells. The cells were diluted to 1mL in LB

media, shaken at 37 °C for 1 hour, and then spread onto LB plates containing 50 μg/mL kanamycin. Plates were incubated overnight at 37 °C, plasmid DNA was isolated from the resulting transformants and screened by sequencing for each mutant variant.

2.2.2: Purification of mutant EF-G

BL-21 DE3 cells containing the pET24b-EFG-His6 variant of interest were grown to mid log (OD_{600}= 0.5) phase in 1L of LB media in a shaking flask at 37 °C, IPTG was added to 0.6 mM, and the cultures were further grown for 3.5 hours. Cells were spun down at 5,000 rpm for 15 minutes at 4 °C and resuspended in 20 mL lysis buffer (50 mM Tris pH 7.8, 100 mM KCl, 6 mM BME, 1 mM EDTA, 1 mM PMSF, and 20 U DNase I) while kept on ice. Cells were lysed by French press twice and centrifuged at 14,000 rpm for 40 minutes at 4 °C. Ni^{2+} resin was washed twice with ddH_2O (double deionized water) and twice with lysis buffer (no EDTA) before being rotated for one hour with the cellular lysate at 4 °C. Resin was applied to a gravity column and washed with 10 column volumes of wash buffer (10 mM Tris pH 7.8, 300 mM KCl, 6 mM BME, and 10 mM imidazole) at 4 °C. Proteins were eluted with 3 mL elution buffer (10 mM Tris pH 7.8, 1 M KCl, 5% glycerol, 6 mM BME, 1 mM EDTA, 300 mM imidazole) at 4 °C. The EF-G proteins were further purified via 4 °C FPLC, using a superdex column and S75 buffer (10 mM Tris pH 7.8, 1 M KCl, 6 mM BME). Peak fractions were dialyzed against 1L storage buffer (50 mM Tris pH 7.8, 50 mM KCl, 10% glycerol, 6 mM BME, 10,000 MWCO) overnight at 4 °C, quantified via Bradford, and stored in small aliquots at -80 °C.

2.2.3: In vitro translation inhibition assays

To determine the IC_{50} of kanamycin and neomycin for each EF-G variant, protein expression using the PURE kit was measured in the presence of AGs. Eight 5 μL in vitro protein synthesis reactions containing aminoglycoside concentrations ranging from 0-7 μM kanamycin or

0-2.5 μM neomycin were used per variant. A master mix was first created by mixing 17 μL solution A, 12.5 μL solution B, 0.8 μL superase RNA inhibitor, 1.7 μL of 12.5 μM EF-G of interest, and 3.2 μL of 0.5 mCi ^{35}S methionine. Next, 4.2 μL of the master mix was aliquoted into eight new microcentrifuge tubes labeled with the appropriate AG. For each aliquot, 0.4 μL AG was added followed by 0.4 μL 125 ng/μL DHFR template. The reactions were incubated for 90 minutes at 37 °C, boiled at 100 °C in the presence of SDS-PAGE buffer for 10 minutes, run on a 10% SDS-PAGE gel, and left in a phosphoscreen overnight for imagining. Band intensity was measured via a typhoon and the application imagequant.

Table 1: Overview of Plasmids Used

Name	Description
pEFG-His6	pET24b containing *E. coli* EF-G-His6
pSM1	pEFG-His6 containing F593L mutation
pSM2	pEFG-His6 containing F605I mutation
pSM3	pEFG-His6 containing F605L mutation
pSM4	pEFG-His6 containing A608E mutation
pSM5	pEFG-His6 containing P610T mutation
pSM6	pEFG-His6 containing P610L mutation

2.3: Results

The *in vitro* PURE system can be used to measure protein synthesis under defined reaction conditions. I ordered a custom PURE system lacking EF-G, enabling me to test the activities of various EF-G proteins in the presence and absence of increasing concentrations of aminoglycosides (figure 2.1). I did this by monitoring the synthesis of DHFR protein in reactions containing ^{35}S methionine. Several initial experiments were performed to determine the ideal final concentration of EF-G (0.5 μM) and incubation time (90 min).

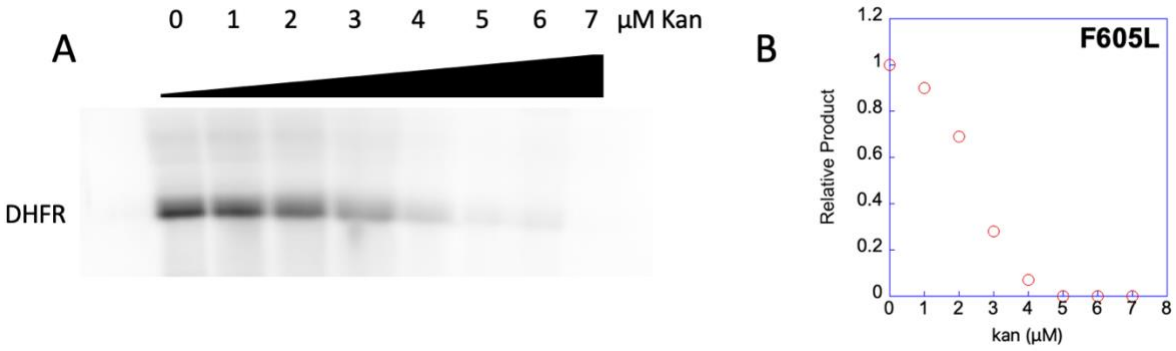

Figure 2.1: Use of the PURE system to measure protein synthesis. (A): 10% SDS polyacrylamide gel containing PURE system reaction exposed overnight in a phosphoscreen. As AG concentrations increase, band intensity decreases. **(B):** Scatterplot of data from a. All data points are normalized against the 0 μM control.

Our first finding was that sub-inhibitory concentrations of aminoglycosides are capable of stimulating translation (figure 2.2-2.3). The observed stimulation was often but not always seen, occurring in about two-thirds of all experiments. When observed, the degree of stimulation was variable, ranging from as little as 20% to nearly 300%. There seems to be no correlation between any one mutation and stimulation or the level of stimulation. The only consistent factor is the concentration at which stimulation occurs. For kanamycin, the stimulation occurs within 0.5-2 μM, while for neomycin the range is 0.25-1 μM. The basis of this stimulation is not entirely clear. However, it is likely due to stabilization of aa-tRNA in the A site by the AG.

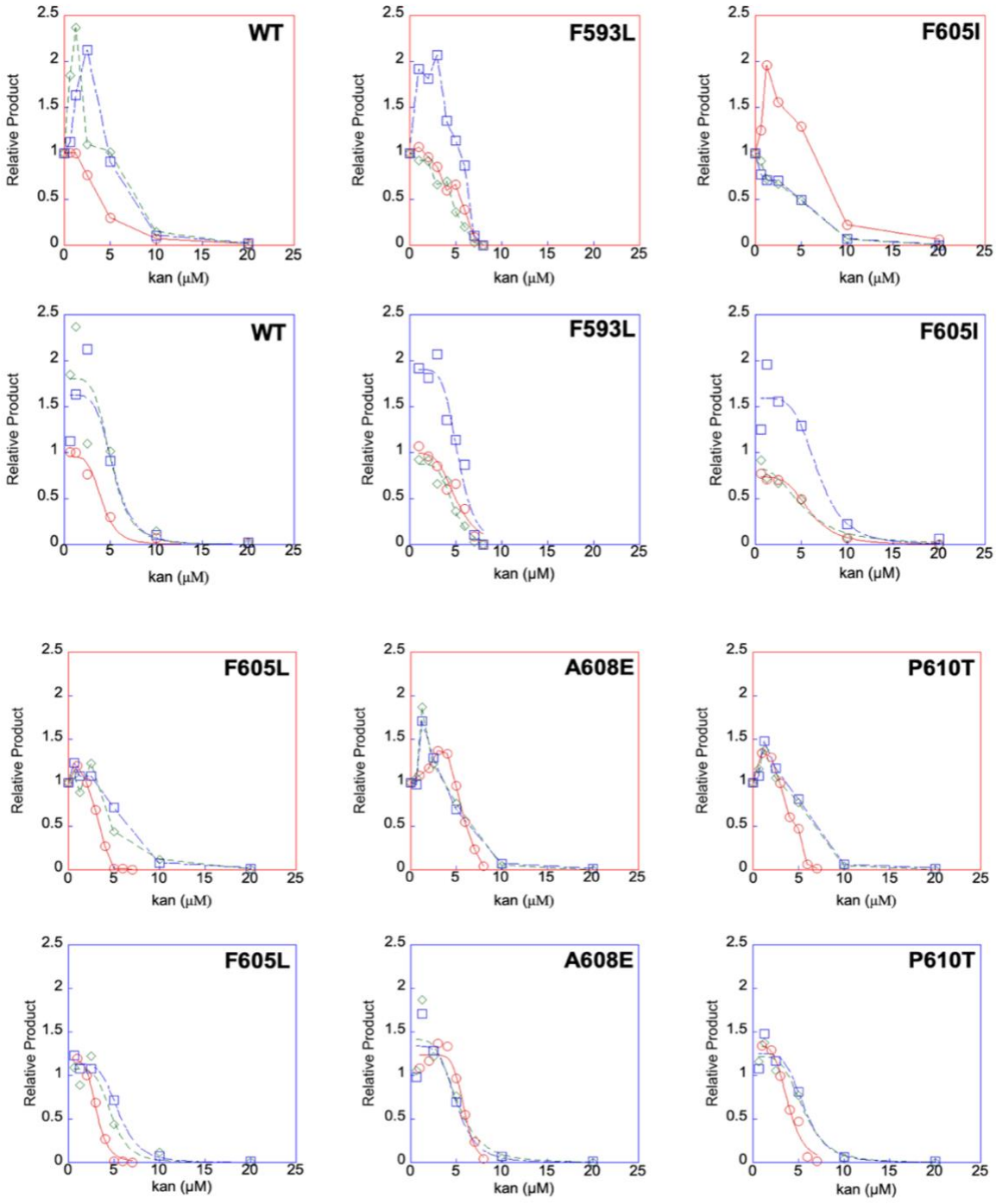

Figure 2.2: Inhibition of translation by kanamycin in the presence of EF-G variants. Plots outlined in red show line graphs with data points connected by straight lines. Plots outlined in blue are fit with a modified dose response equation to calculate the IC_{50} values.

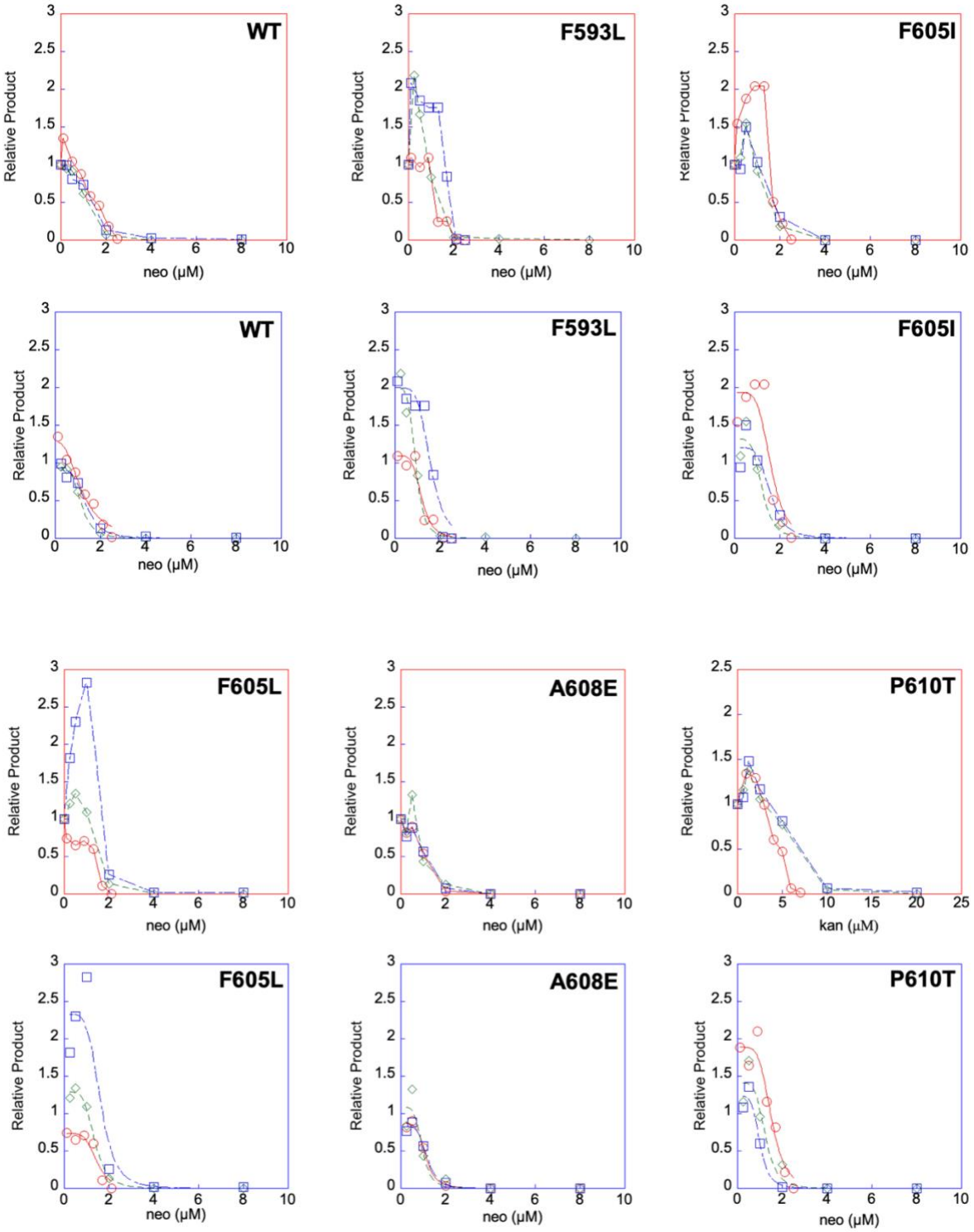

Figure 2.3: Inhibition of translation by neomycin in the presence of EF-G variants. Plots outlined in red show line graphs with data points connected by straight lines. Plots outlined in blue are fit with a modified dose response equation to calculate the IC_{50} values.

In order to calculate IC_{50} values, I fit the data to the modified dose-response equation $y=c(1/((1+(x/b)^a)))$, where *a* equals the Hill Coefficient, *b* represents the IC_{50} value, and *c* represents the maximal product produced. This relatively simple equation does not fit the apparent increase in translation at subinhibitory AG concentrations, but can deduce the IC_{50} reliably (figures 2.1-2.2 and tables 2-3). Data from those reactions containing AGs (> 0 μM) were used for the curve fitting. In rare cases, a clearly erroneous fit was obtained with the Hill Coefficient greater than 10. This occurred in the following replicates: the blue WT kanamycin, the green F605L kanamycin, the red F605I neomycin, the blue F605L neomycin, the green A608E neomycin, and the blue P610T neomycin. In these cases, the Hill Coefficient was set as 5 and the data were refit. This did not substantially change the IC_{50} and provided a more reasonable curve, consistent with the other replicates.

Table 2. Inhibition of translation by kanamycin in the presence of various EF-G mutants

Mutant	Mean IC_{50} (μM)[1]	P-value[2]	Average Hill Coefficient
WT	4.9 ± 0.4	N/A	2.4
F593L	5.0 ± 0.2	0.35	5.3
F605I	5.0 ± 0.5	0.43	3.8
F605L	4.6 ± 0.7	0.47	4.9
A608E	5.4 ± 0.3	0.36	5.9
P610T	5.0 ± 0.6	0.41	4.5

Table 3. Inhibition of translation by neomycin in the presence of various EF-G mutants

Mutant	Mean IC_{50} (μM)[1]	P-value[2]	Average Hill Coefficient[3]
WT	1.2 ± 0.1	N/A	3.8
F593L	1.2 ± 0.1	0.48	9.2
F605I	1.5 ± 0.1	0.48	4.5
F605L	1.5 ± 0.1	0.45	9.4
A608E	1.1 ± 0.1	0.42	5.7
P610T	1.3 ± 0.2	0.47	4.7

[1]Data represent mean ± SEM for ≥ 3 independent experiments.
[2]A two-tailed t test was used to assess differences from the WT. No differences were deemed significant.
[3] The average value of Hill Coefficients that were not manually set to 5.

No significant difference in IC_{50} was seen between the wild type and any EF-G mutant for either kanamycin or neomycin. This appears to contradict the *in vivo* data, which shows 2- to 4-fold increases in MIC conferred by these mutations.

2.4: Discussion

One unexpected finding of this study is that translation in the PURE system is stimulated by low concentrations of AGs. While I could not find another example of AG-induced stimulation of translation in the literature, this effect is likely related to the fact that AGs stabilize binding of A-site tRNA[34]. For example, the AGs may promote decoding and hence speed the elongation cycle. In *E. coli* cells, total tRNA concentration varies from 200 to 360 μM depending on how fast the cell is replicating[45]. The PURE system contains a somewhat lower total tRNA concentration of 3.5 mg/mL or 140 μM. I suggest that these lower tRNA concentrations slow decoding and limit the overall rate of translation. Subinhibitory concentrations of AGs may speed this step of elongation substantially and hence increase the overall rate. Puzzlingly, the observed stimulation is variable. In one third of all experiments, no stimulation was seen, and instead only inhibition was observed. This variability appears random, as it is not confined to any specific EF-G variants. Perhaps slight differences between reaction conditions explain this variability.

My initial hypothesis was that the point mutations in domain 4 of EF-G were directly responsible for the resistance seen *in vivo*. I believed that through an unknown mechanism, these mutant forms of EF-G disrupt AG-ribosome hydrogen bonding, ejecting the AG akin to the mechanism of Tet-O. Due to their high degree of sequence homology, similar structure, and common GTPase activity, this was not an unreasonable hypothesis. The fact that these mutations confer resistance to aminoglycosides *in vivo* but not *in vitro* presents an apparent paradox.

How can these data be explained? One possibility is that cells containing mutant EF-G proteins express EF-G at a higher rate. Since EF-G concentrations are controlled in the PURE system, any effect dependent on high EF-G concentrations will not be seen. While possible, this scenario seems unlikely as the PURE system experiences clear translation inhibition in the presence of AGs.

The simplest explanation is that these EF-G mutations confer resistance through an indirect mechanism. One way for a mutation to confer indirect antibiotic resistance would be by altering gene expression. In the case of EF-G, indirect resistance may arise in the following manner. The mutant EF-G causes a defect in translocation, which causes ribosome traffic on some mRNAs more than others, inducing global perturbations of gene expression. Increased and or decreased expression of certain genes may be responsible for conferred resistance *in vivo*. For instance, if general transporters were upregulated they may allow the cell to pump AGs out at a faster rate. Alternatively, the downregulation of proteins mediating the permeability of the cell envelope might slow movement of the AG into the cell. There is precedence for translation defects to perturb gene expression globally. For example, loss of LepA, an EF-G analog, alters initiation of translation and consequently causes widespread changes in gene expression[46].

Evolution experiments suggest that high-level AG resistance requires several steps. In these experiments, mutations in *fusA* (EF-G) tend to arise first, followed by mutations in *ptsP* (a nitrogen metabolism phosphotransferase), *fhuA* (an outer membrane transporter responsible for ferrichrome-iron and albomycin transport), and the *potABCD* (polyamine oligo-transport) operon[42,43]. Overproduction of these proteins could hypothetically confer low levels of AG resistance, as they are related to known AG resistance proteins. For example, aminoglycoside phosphotransferases have evolved from other phosphotransferases to deactivate AGs, while *fhuA* and *potABCD* encode transporters capable of removing antibiotics from the cell. Perhaps the observed resistance *in vivo* is due to the EF-G variants perturbing gene expression in such a way that these proteins are overproduced. Secondary mutations in these proteins then provide a higher level of AG resistance in further evolved strains. This scenario can explain how resistance is acquired in a stepwise manner and why EF-G variants provide no resistance *in vitro*.

In order to investigate whether the mutant EF-Gs are capable of indirectly conferring resistance to AGs, ribosome profiling should be performed on cells containing either WT or mutant EF-G. If there is a significant difference on the average ribosome density then there is evidence that the mutant EF-G can alter translation. Changes in RNA-seq coverage would show other potential secondary effects on mRNA production and or degradation. One could then predict which genes were being over or under expressed and explore their potential role in resistance. As the *potABCD*, *fhuA*, and *ptsP* genes are known targets of mutations after *fusA*, characterizing strains with either the WT or mutant proteins should provide insight into their specific roles in AG resistance.

References

(1) Schmeing, T. M.; Ramakrishnan, V. What Recent Ribosome Structures Have Revealed about the Mechanism of Translation. *Nature* **2009**, *461* (7268), 1234–1242. https://doi.org/10.1038/nature08403.

(2) Yusupova, G.; Yusupov, M. Ribosome Biochemistry in Crystal Structure Determination. *RNA* **2015**, *21* (4), 771–773. https://doi.org/10.1261/rna.050039.115.

(3) Qin, D.; Abdi, N. M.; Fredrick, K. Characterization of 16S RRNA Mutations That Decrease the Fidelity of Translation Initiation. *RNA* **2007**, *13* (12), 2348–2355. https://doi.org/10.1261/rna.715307.

(4) Shine, J.; Dalgarno, L. Terminal-Sequence Analysis of Bacterial Ribosomal RNA. Correlation between the 3'-Terminal-Polypyrimidine Sequence of 16-S RNA and Translational Specificity of the Ribosome. *Eur. J. Biochem.* **1975**, *57* (1), 221–230. https://doi.org/10.1111/j.1432-1033.1975.tb02294.x.

(5) Shine, J.; Dalgarno, L. The 3′-Terminal Sequence of Escherichia Coli 16S Ribosomal RNA: Complementarity to Nonsense Triplets and Ribosome Binding Sites. *Proc. Natl. Acad. Sci. U. S. A.* **1974**, *71* (4), 1342–1346.

(6) Milon, P.; Carotti, M.; Konevega, A. L.; Wintermeyer, W.; Rodnina, M. V.; Gualerzi, C. O. The Ribosome-Bound Initiation Factor 2 Recruits Initiator TRNA to the 30S Initiation Complex. *EMBO Rep.* **2010**, *11* (4), 312–316. https://doi.org/10.1038/embor.2010.12.

(7) Carter, A. P.; Clemons, W. M.; Brodersen, D. E.; Morgan-Warren, R. J.; Hartsch, T.; Wimberly, B. T.; Ramakrishnan, V. Crystal Structure of an Initiation Factor Bound to the 30S Ribosomal Subunit. *Science* **2001**, *291* (5503), 498–501. https://doi.org/10.1126/science.1057766.

(8) Structural basis of sequestration of the anti-Shine-Dalgarno sequence in the Bacteroidetes ribosome | Nucleic Acids Research | Oxford Academic https://academic.oup.com/nar/article/49/1/547/6039927 (accessed 2022 -01 -13).

(9) Antoun, A.; Pavlov, M. Y.; Andersson, K.; Tenson, T.; Ehrenberg, M. The Roles of Initiation Factor 2 and Guanosine Triphosphate in Initiation of Protein Synthesis. *EMBO J.* **2003**, *22* (20), 5593–5601. https://doi.org/10.1093/emboj/cdg525.

(10) Agirrezabala, X.; Frank, J. Elongation in Translation as a Dynamic Interaction among the Ribosome, TRNA, and Elongation Factors EF-G and EF-Tu. *Q. Rev. Biophys.* **2009**, *42* (3), 159–200. https://doi.org/10.1017/S0033583509990060.

(11) Ninio, J. Multiple Stages in Codon-Anticodon Recognition: Double-Trigger Mechanisms and Geometric Constraints. *Biochimie* **2006**, *88* (8), 963–992. https://doi.org/10.1016/j.biochi.2006.06.002.

(12) MOORE, P. B.; STEITZ, T. A. After the Ribosome Structures: How Does Peptidyl Transferase Work? *RNA* **2003**, *9* (2), 155–159. https://doi.org/10.1261/rna.2127103.

(13) Zhou, J.; Lancaster, L.; Donohue, J. P.; Noller, H. F. Spontaneous Ribosomal Translocation of MRNA and TRNAs into a Chimeric Hybrid State. *Proc. Natl. Acad. Sci.* **2019**, *116* (16), 7813–7818. https://doi.org/10.1073/pnas.1901310116.

(14) Chen, C.; Cui, X.; Beausang, J. F.; Zhang, H.; Farrell, I.; Cooperman, B. S.; Goldman, Y. E. Elongation Factor G Initiates Translocation through a Power Stroke. *Proc. Natl. Acad. Sci.* **2016**, *113* (27), 7515–7520. https://doi.org/10.1073/pnas.1602668113.

(15) Jurnak, F. The ABC of EF-G. *Struct. Lond. Engl. 1993* **1994**, *2* (9), 785–788. https://doi.org/10.1016/s0969-2126(94)00078-6.

(16) Macé, K.; Giudice, E.; Chat, S.; Gillet, R. The Structure of an Elongation Factor G-Ribosome Complex Captured in the Absence of Inhibitors. *Nucleic Acids Res.* **2018**, *46* (6), 3211–3217. https://doi.org/10.1093/nar/gky081.
(17) Carbone, C. E.; Loveland, A. B.; Gamper, H. B.; Hou, Y.-M.; Demo, G.; Korostelev, A. A. Time-Resolved Cryo-EM Visualizes Ribosomal Translocation with EF-G and GTP. *Nat. Commun.* **2021**, *12* (1), 7236. https://doi.org/10.1038/s41467-021-27415-0.
(18) Shoji, S.; Walker, S. E.; Fredrick, K. Ribosomal Translocation: One Step Closer to the Molecular Mechanism. *ACS Chem. Biol.* **2009**, *4* (2), 93–107. https://doi.org/10.1021/cb8002946.
(19) Nakamura, Y.; Ito, K.; Isaksson, L. A. Emerging Understanding of Translation Termination. *Cell* **1996**, *87* (2), 147–150. https://doi.org/10.1016/S0092-8674(00)81331-8.
(20) Seit-Nebi, A.; Frolova, L.; Justesen, J.; Kisselev, L. Class-1 Translation Termination Factors: Invariant GGQ Minidomain Is Essential for Release Activity and Ribosome Binding but Not for Stop Codon Recognition. *Nucleic Acids Res.* **2001**, *29* (19), 3982–3987. https://doi.org/10.1093/nar/29.19.3982.
(21) Adio, S.; Sharma, H.; Senyushkina, T.; Karki, P.; Maracci, C.; Wohlgemuth, I.; Holtkamp, W.; Peske, F.; Rodnina, M. V. Dynamics of Ribosomes and Release Factors during Translation Termination in E. Coli. *eLife* **2018**, *7*, e34252. https://doi.org/10.7554/eLife.34252.
(22) Zhou, J.; Lancaster, L.; Trakhanov, S.; Noller, H. F. Crystal Structure of Release Factor RF3 Trapped in the GTP State on a Rotated Conformation of the Ribosome. *RNA* **2012**, *18* (2), 230–240. https://doi.org/10.1261/rna.031187.111.
(23) Kiel, M. C.; Kaji, H.; Kaji, A. Ribosome Recycling: An Essential Process of Protein Synthesis. *Biochem. Mol. Biol. Educ.* **2007**, *35* (1), 40–44. https://doi.org/10.1002/bmb.6.
(24) Savelsbergh, A.; Rodnina, M. V.; Wintermeyer, W. Distinct Functions of Elongation Factor G in Ribosome Recycling and Translocation. *RNA* **2009**, *15* (5), 772–780. https://doi.org/10.1261/rna.1592509.
(25) Fu, Z.; Kaledhonkar, S.; Borg, A.; Sun, M.; Chen, B.; Grassucci, R. A.; Ehrenberg, M.; Frank, J. Key Intermediates in Ribosome Recycling Visualized by Time-Resolved Cryo-Electron Microscopy. *Struct. Lond. Engl. 1993* **2016**, *24* (12), 2092–2101. https://doi.org/10.1016/j.str.2016.09.014.
(26) Chen, Y.; Kaji, A.; Kaji, H.; Cooperman, B. S. The Kinetic Mechanism of Bacterial Ribosome Recycling. *Nucleic Acids Res.* **2017**, *45* (17), 10168–10177. https://doi.org/10.1093/nar/gkx694.
(27) Peske, F.; Rodnina, M. V.; Wintermeyer, W. Sequence of Steps in Ribosome Recycling as Defined by Kinetic Analysis. *Mol. Cell* **2005**, *18* (4), 403–412. https://doi.org/10.1016/j.molcel.2005.04.009.
(28) Julián, P.; Konevega, A. L.; Scheres, S. H. W.; Lázaro, M.; Gil, D.; Wintermeyer, W.; Rodnina, M. V.; Valle, M. Structure of Ratcheted Ribosomes with TRNAs in Hybrid States. *Proc. Natl. Acad. Sci.* **2008**, *105* (44), 16924–16927. https://doi.org/10.1073/pnas.0809587105.
(29) Li, W.; Trabuco, L. G.; Schulten, K.; Frank, J. Molecular Dynamics of EF-G during Translocation. *Proteins* **2011**, *79* (5), 1478–1486. https://doi.org/10.1002/prot.22976.
(30) Margus, T.; Remm, M.; Tenson, T. A Computational Study of Elongation Factor G (EFG) Duplicated Genes: Diverged Nature Underlying the Innovation on the Same Structural Template. *PLOS ONE* **2011**, *6* (8), e22789. https://doi.org/10.1371/journal.pone.0022789.

(31) Guo, Z.; Noller, H. F. Rotation of the Head of the 30S Ribosomal Subunit during MRNA Translocation. *Proc. Natl. Acad. Sci.* **2012**, *109* (50), 20391–20394. https://doi.org/10.1073/pnas.1218999109.
(32) Ermolenko, D. N.; Noller, H. F. MRNA Translocation Occurs during the Second Step of Ribosomal Intersubunit Rotation. *Nat. Struct. Mol. Biol.* **2011**, *18* (4), 457–462. https://doi.org/10.1038/nsmb.2011.
(33) Zhou, J.; Lancaster, L.; Donohue, J. P.; Noller, H. F. How the Ribosome Hands the A-Site TRNA to the P Site During EF-G-Catalyzed Translocation. *Science* **2014**, *345* (6201), 1188–1191. https://doi.org/10.1126/science.1255030.
(34) Ying, L.; Zhu, H.; Shoji, S.; Fredrick, K. Roles of Specific Aminoglycoside-Ribosome Interactions in the Inhibition of Translation. *RNA N. Y. N* **2019**, *25* (2), 247–254. https://doi.org/10.1261/rna.068460.118.
(35) Borovinskaya, M. A.; Pai, R. D.; Zhang, W.; Schuwirth, B. S.; Holton, J. M.; Hirokawa, G.; Kaji, H.; Kaji, A.; Cate, J. H. D. Structural Basis for Aminoglycoside Inhibition of Bacterial Ribosome Recycling. *Nat. Struct. Mol. Biol.* **2007**, *14* (8), 727–732. https://doi.org/10.1038/nsmb1271.
(36) Cabañas, M. J.; Vázquez, D.; Modolell, J. Inhibition of Ribosomal Translocation by Aminoglycoside Antibiotics. *Biochem. Biophys. Res. Commun.* **1978**, *83* (3), 991–997. https://doi.org/10.1016/0006-291x(78)91493-6.
(37) Jo, J. T. H.; Brinkman, F. S. L.; Hancock, R. E. W. Aminoglycoside Efflux in Pseudomonas Aeruginosa: Involvement of Novel Outer Membrane Proteins. *Antimicrob. Agents Chemother.* **2003**, *47* (3), 1101–1111. https://doi.org/10.1128/AAC.47.3.1101-1111.2003.
(38) Smith, C. A.; Baker, E. N. Aminoglycoside Antibiotic Resistance by Enzymatic Deactivation. *Curr. Drug Targets Infect. Disord.* **2002**, *2* (2), 143–160. https://doi.org/10.2174/1568005023342533.
(39) Soucy, S. M.; Huang, J.; Gogarten, J. P. Horizontal Gene Transfer: Building the Web of Life. *Nat. Rev. Genet.* **2015**, *16* (8), 472–482. https://doi.org/10.1038/nrg3962.
(40) Li, W.; Atkinson, G. C.; Thakor, N. S.; Allas, Ü.; Lu, C.; Chan, K.-Y.; Tenson, T.; Schulten, K.; Wilson, K. S.; Hauryliuk, V.; Frank, J. Mechanism of Tetracycline Resistance by Ribosomal Protection Protein Tet(O). *Nat. Commun.* **2013**, *4* (1), 1477. https://doi.org/10.1038/ncomms2470.
(41) Connell, S. R.; Trieber, C. A.; Dinos, G. P.; Einfeldt, E.; Taylor, D. E.; Nierhaus, K. H. Mechanism of Tet(O)-Mediated Tetracycline Resistance. *EMBO J.* **2003**, *22* (4), 945–953. https://doi.org/10.1093/emboj/cdg093.
(42) Parallel Evolution of Tobramycin Resistance across Species and Environments | mBio https://journals.asm.org/doi/10.1128/mBio.00932-20 (accessed 2022 -01 -13).
(43) Ibacache-Quiroga, C.; Oliveros, J. C.; Couce, A.; Blázquez, J. Parallel Evolution of High-Level Aminoglycoside Resistance in Escherichia Coli Under Low and High Mutation Supply Rates. *Front. Microbiol.* **2018**, *9*, 427. https://doi.org/10.3389/fmicb.2018.00427.
(44) Mogre, A.; Sengupta, T.; Veetil, R. T.; Ravi, P.; Seshasayee, A. S. N. Genomic Analysis Reveals Distinct Concentration-Dependent Evolutionary Trajectories for Antibiotic Resistance in Escherichia Coli. *DNA Res. Int. J. Rapid Publ. Rep. Genes Genomes* **2014**, *21* (6), 711–726. https://doi.org/10.1093/dnares/dsu032.
(45) Co-variation of tRNA Abundance and Codon Usage in Escherichia coli at Different Growth Rates | Elsevier Enhanced Reader https://reader.elsevier.com/reader/sd/pii/S0022283696904283?token=40464FAB00D7D855

9D262C07D83DE4F76B70CC0F23B6D7D19D3B74F3C38BFDC7171CF3A511CF0767C905E8ECD2CC11AA&originRegion=us-east-1&originCreation=20220307023643 (accessed 2022 -03 -06). https://doi.org/10.1006/jmbi.1996.0428.

(46) Balakrishnan, R.; Oman, K.; Shoji, S.; Bundschuh, R.; Fredrick, K. The Conserved GTPase LepA Contributes Mainly to Translation Initiation in Escherichia Coli. *Nucleic Acids Res.* **2014**, *42* (21), 13370–13383. https://doi.org/10.1093/nar/gku1098.